# Spatiotemporal variations of snow characteristics in Xinjiang, China over 1961–2013

Yang Ding, Yi Li, Linchao Li, Ning Yao, Wei Hu, Daqing Yang and Chunyan Chen

## ABSTRACT

Daily snow data during 1961–2013 at the 105 meteorological stations in Xinjiang, China were used to investigate the spatiotemporal variations of several parameters, including starting and ending dates, duration, annual and monthly average and maximum snow depths. The modified Mann–Kendall test, empirical mode decomposition, empirical orthogonal function (EOF), and the inverse distance weight interpolation were applied. Snow lasted for 71 to 120 days. Snow depth decreased from north to south. Daily snow depth had periodical variations and were classified as four typical types, i.e., flat peak, multi-peak, sharp single-peak, and right-skewed. After daily snow depth was decomposed into 17 intrinsic mode functions (IMFs), IMF9, IMF10, and IMF11 over 189, 302, and 437 days of scales accounted for 79% of the total spatiotemporal variance in snow depth. Both annual starting and ending day numbers had decreasing trends, while the duration in days had an increasing trend. The average and maximum snow depth increased in most sites whether considering the seasonality in December, January, February, or annual values. EOF1 accounted for 70% of spatial variability and the temporal coefficient EC1 varied periodically. The spatiotemporal analysis of snow properties provides a basis for snowmelt understanding.

**Key words** | Mann–Kendall test, snow cover duration, snow depth, spatiotemporal variation

**Yang Ding**
**Yi Li** (corresponding author)
**Linchao Li**
**Ning Yao**
College of Water Resources and Architecture Engineering,
Northwest A&F University,
Yangling 712100, China
E-mail: *liyi@nwsuaf.edu.cn*

**Yi Li**
**Linchao Li**
Key Laboratory of Agricultural Soil and Water Engineering in Arid and Semiarid Areas, Ministry of Education,
Northwest A&F University,
Yangling 712100, China

**Wei Hu**
New Zealand Institute for Plant & Food Research Limited,
Private Bag 4704, Christchurch 8140, New Zealand

**Daqing Yang**
National Hydrology Research Center,
Saskatoon S7N 3H5, Canada

**Chunyan Chen**
Xinjiang Meteorological Observatory,
Urumqi 830002, China

## INTRODUCTION

Snow cover is an important component of the hydrosphere and it reaches 46 million km$^2$ during winter in the northern hemisphere (Frei & Robinson 1999). Wintertime snow and spring snowmelt are critical to agriculture, ecosystem, and water resources management in cold regions. Snowpack is a special land cover type, and it is a key factor for local and global scales climate change in response to global warming (Liston 1999; Frei & Gong 2005; Bavay *et al.* 2009). Snow depth is an indispensable indicator for estimating snow water equivalent, calculating surface radiation and water budget, and simulating snowmelt runoff in spring. The high reflectivity and the low conductivity of snowpack affect the energy exchange within the land–atmosphere system (Lamb 1955; Namias 1964; Hahn & Shukla 1976; Dey & Kumar 1983; Foster *et al.* 1983).

Many studies have used ground observations and data to analyze long-term changes in snow depth, to reveal its variation and relationship with the other meteorological variables, and to predict future changes by different snow models (Pomeroy *et al.* 2007; Wu & Kirtman 2007; Jin & Wen 2012; Tang *et al.* 2013). In recent years, snow cover variations have not only been observed by the routine surface meteorological observation, but also with other advanced technologies, such as hyper-spectral, microwave radiometry, and remote sensing (Rango *et al.* 1989; Wang *et al.* 1992; Rott & Nagler 1995; Grody & Basist 1996; Tait & Armstrong

doi: 10.2166/nh.2017.035

1996; Butt 2006; Butt & Kelly 2008). These technologies were applied successfully for snow monitoring, but the underlying surface is complex, and there is still a need for ground observation and data to retrieve snow properties. Moreover, snow observation and data are also vital for regional climate change, snowmelt modeling, and snowmelt floods. Stable snow cover areas in China are mainly located in the Tibet Plateau, the north Xinjiang Tianshan Mountains area, and the northeast three provinces Inner Mongolia region (Li & Mi 1983). The changes in snow depth affect snowmelt processes, which is important for water resources in the arid and semi-arid area of Xinjiang Autonomous region (Shen *et al.* 2013).

Spatiotemporal variability analysis involves the multivariate spatial analysis methods for hydrological time series, e.g., singular value decomposition (Wang *et al.* 2017), canonical correlation (Hardoon *et al.* 2004), cluster analysis (Nauditt *et al.* 2017), empirical mode decomposition (EMD), and empirical orthogonal functions (EOFs) (Hu *et al.* 2017), etc. EOF analysis is a widely applied statistical method for analyzing large multidimensional datasets (Perry & Niemann 2007). The EOF approach can condense the spatiotemporal information, study spatial and systematic structures, and identify dominant patterns of variations inherent at the measuring sites. To the present, the EOF method has been applied to analyze soil water content in the Canadian Prairie pothole region (Hu & Si 2016), terrestrial water storage in the Tarim River basin (Yang *et al.* 2017), water quality variation of Nakdong River, Korea (Sung *et al.* 2017), and many other water-related properties for different regions (Cerrone *et al.* 2017; Deepthi *et al.* 2017), but has not been widely used for spatiotemporal variability analysis of snow-related properties in Xinjiang, China. In addition, the EMD decomposes the overall spatial pattern into a finite and often small number of intrinsic modes, which are known as intrinsic mode functions (IMFs) that represent the characteristic scales of variability in the physical property.

This research aims to analyze the spatiotemporal variations of snow parameters, including snow cover starting date ($D_s$), ending date ($D_e$), duration ($D_d$), seasonal average snow depth ($SD_{avr}$), and maximum snow depth ($SD_{max}$). The snow depth data at 105 sites in Xinjiang, China, over the period 1961–2013 were collected. The seasonal trends, scales, and spatiotemporal variability of $D_s$, $D_e$, $D_d$, $SD_{avr}$, and $SD_{max}$ have been investigated to illustrate the overall changes of snow cover.

## MATERIALS AND METHODS

### Study area and datasets

The Xinjiang Uygur Autonomous region is located in northwestern China with a longitude range of 73°40′E–96°23′E and altitude range of 34°22′N–49°10′N. The longest distance from east to west is 1,900 km, and from north to south is 1,500 km. The area of Xinjiang is about 1,660,000 km$^2$, about one-sixth of the total area of China. The border of Xinjiang region is 5,300 m, which is the longest border in the provincial regions in China. Xinjiang has a temperate continental climate and is a typical arid and semi-arid region, being characterized by 'three mountains (i.e., the Kunlun Mountains in the south, the Tianshan Mountains in central Xinjiang, and the Altai Mountains in the northeast) and two basins (i.e., Zhungaer and Tulufan)' (Li *et al.* 2017a, 2017b). There is a long, dry, and cold winter, and a short, dry, and hot summer. Annual mean precipitation is 145 mm, and evaporation capacity is about 200 mm. According to the climatic conditions, Xinjiang is divided into different sub-regions, i.e., north, south, and Tianshan Mountains area. The snowfall in north Xinjiang and Tianshan Mountains area accounts for about one-third of the annual precipitation, which is vital for water resources utilization in Xinjiang.

The daily snow data for the period 1961–2013 at the 105 stations in Xinjiang (Figure 1) were obtained from Xinjiang Meteorology Bureau, Urumqi, China. The elevations of these selected sites range between −197 and 8,494 m above sea level. The snow properties were measured and recorded manually. Snow depth was measured with a ruler, depth was measured three times to provide an average value. The snow data have undergone strict quality controls by Xinjiang Meteorological Observatory with 99.9% completeness. Missing data were replaced by the long-term averages for the neighboring days.

The snow cover parameters including $D_s$, $D_e$, $D_d$, $SD_{avr}$, and $SD_{max}$ were analyzed to show snow variations. For easy statistical calculation, both $D_s$ and $D_e$ values were counted from July 1st, if daily snow depth is $\geq$1 cm, $D_d$ increased

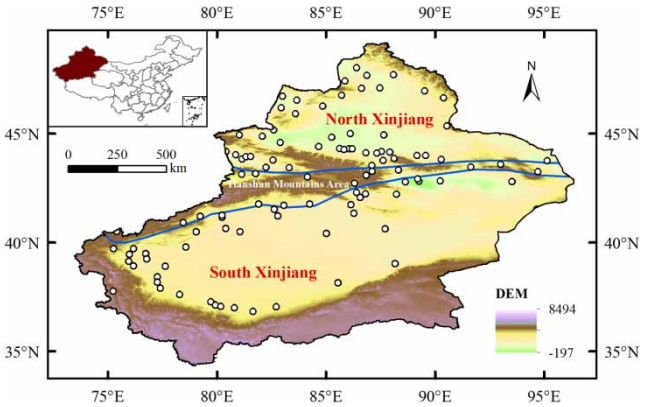


**Figure 1** | The geographical location and elevations (Unit: m) of the selected 105 weather stations in Xinjiang, China. The lines represent the borders of north Xinjiang, Tianshan-mountains-area and south Xinjiang.

by 1. If the snow lasted longer than 5 days, it belongs to a stable snow cover year (Wang *et al.* 2014). The $D_d$ within the stable snow cover year is equal to $D_e$ minus $D_s$.

## Empirical mode decomposition

EMD separates the variations in snow parameters according to their characteristic scales. EMD works directly in the temporal domain with the basis derived from the data. In a natural system, the overall variability is controlled by a number of processes occurring together at different intensities or scales (Goovaerts 1998). The processes with similar scales are separated into different IMFs. In defining the IMFs, they should satisfy the following conditions: (i) the mode might be linear and the number of minima or maxima and zero crossings must either be equal or differ at most by one, while zero crossing indicates the point where the function changes sign; (ii) the oscillation will be symmetric with respect to the local mean. According to these definitions, IMFs can be obtained after decomposing any function through a sifting process.

## Trend test

The modified Mann–Kendall (MMK) method (Yue & Wang 2002) based on a non-parametric analysis (Mann 1945; Kendall 1975) was applied in this study to robustly test the trend in the time series $x_L$ ($L = 1, 2, \ldots, 53$ years). The MMK statistic $Z_M$ considers the effects of self-correlation on original Mann–Kendall statistic ($Z$) using a correction factor – $n^s$ (Li *et al.* 2010), written as follows:

$$Z_M = Z/\sqrt{n^s},$$

where

$$n^s = \begin{cases} 1 + \dfrac{2}{n}\displaystyle\sum_{j=1}^{n-1}(n-1)r_j & \text{for } j > 1 \\ 1 + 2\dfrac{r_1^{n+1} - nr_1^2 + (n-1)r_1}{n(r_1-1)^2} & \text{for } j = 1 \end{cases} \quad (1)$$

where $r_j$ is self-correlation coefficient of $x_L$ given a lag time $j$ (Kottegoda 1980; Topaloglu 2006). If $r_j$ falls inside the confidence limits, the hypothesis that $r_j$ is zero is accepted using a two-tailed test and a maximal lag $j$ with temporal-dependence in $x_L$, denoted as $j_{TD}$, is determined.

The magnitude of the trend ($b$) was estimated by Sen (1968), written as follows:

$$b = Median\left(\frac{x_k - x_m}{k - m}\right), \text{ for all of } m < k \quad (2)$$

where $x_m$ and $x_k$ are the values in the $m$th and $k$th year, respectively.

The trend test for annual time series cannot show seasonality, therefore a trend test for a seasonal dataset is also conducted for December, January, and February when snow cover lasts for the whole month. The detailed procedure for seasonal trend test is referred to in Helsel & Hirsch (2002).

## Variation coefficient

The variability of the snow cover characteristics was quantified with the coefficient of variation ($C_v$), calculated with the following equation (Nielsen & Bouma 1985):

$$C_v = \frac{\sigma}{\overline{x_L}} \quad (3)$$

where $\sigma$ and $\overline{x_L}$ are standard deviation and mean value of the data series $x_L$, respectively. Variability levels were classified as weak, moderate, or strong with $C_v \leq 0.1$, $0.1 < C_v < 1.0$ and $C_v \geq 1.0$, respectively.

### Empirical orthogonal function

The EOF linearly transforms original series to a substantial smaller set of uncorrelated variables, which can still represent most information of the original series (North *et al.* 1982). Using EOF, snow depth time series can be decomposed into a temporal mean (i.e., time-stable pattern, $M_{tn}$) and a temporal anomaly ($A_{tn}$), which is directly related to snow depth dynamics. The $A_{tn}$ is further decomposed into a space-invariant temporal anomaly ($A_{tnt}$) and a space-variant temporal anomaly ($R_{tnt}$). The $R_{tnt}$ is responsible for spatial variability of snow depth dynamics and is further decomposed into the sum of product of spatial structures and temporally varying coefficients (ECs) using EOF (Perry & Niemann 2007; Hu & Si 2016). Snow depth at location $n$ and time $t$ ($S_{tn}$) can be separated into:

$$S_{tn} = M_{tn} + A_{tn} + R_{tn} \tag{4}$$

$R_{tn}$ can be expressed as:

$$R_{tn} = \sum \mathrm{EOF} \times \mathrm{EC}^{\mathrm{T}} \tag{5}$$

The ECs correspond to the eigenvectors of the matrix of spatial covariance of the $R_{tn}$. By projecting the $R_{tn}$ onto the matrix ECs, the EOFs can be obtained: EOFs = $R_{tn}$ ECs. The number of EOF (or EC) series equals the number of sampling dates. Usually, a substantial amount of variance can be explained by a small number of EOFs. The significance of EOFs is determined at a 95% confidence level.

Spatial distributions of the snow parameters, trends, and the EOFs were obtained by the inverse distance weight interpolation method in ArcMap 10.2 software.

## RESULTS AND DISCUSSION

### Characteristics of variations for annual and inter-annual snow depth

There was a total of 105 sites. The Jimunai station in north Xinjiang was taken as an example. Figure 2 shows temporal variations of observed, IMFs, and variances in percentages for daily snow depth during 1961–2013 at Jimunai. Snow depth fluctuated periodically with different peaks for each year (Figure 2(a)). There was a $SD_{max}$ of 75 cm in 2010 and a minimum of 0 cm each year. Snowfall was concentrated from October to February. The variances over different IMFs varied (Figure 2(b) and 2(c)). About 79.6% of the total variation of snow depth was separated in IMF9 (scale of 189 days), IMF10 (scale of 302 days), and IMF11 (scale of 437 days), respectively; the scale was about half (for IMF9) or one year (for IMF10 and IMF11). These scales corresponded to the period of climate variations. Therefore, variations of snow depth were determined by the vibrations of IMF9, IMF10, and IMF11. The residual line tended to increase from the 1980s, indicating a general increase of snow depth after the 1980s.

Daily snow depth at the other 104 stations in Xinjiang showed similar seasonal changes and scales but with different ranges. $SD_{avr}$ was in the range of 6.3–21.3 cm for north Xinjiang, 4.2–10.8 cm for Tianshan Mountains area, 1.5–5.0 cm for south Xinjiang, and 4.8–12.8 cm for the whole of Xinjiang, respectively. $SD_{max}$ was in the range of 13.1–42.5 cm for north Xinjiang, 11.8–23.6 cm for Tianshan Mountains area, 2.0–8.9 cm for south Xinjiang, and 10.3–25.4 cm for the whole of Xinjiang, respectively.

Four common types of snow depth curve (Chen *et al.* 2015) were classified to show daily snow depth variations within the year at Jimunai station (Figure 3). The flat peak, multi-peak, sharp single-peak, and right-skewed types, corresponding to Figure 3(a), 3(b), 3(c) and 3(d), occurred 18, 15, 10, and 9 times at Jimunai, respectively.

Curve types for daily snow depth at the other 104 stations in Xinjiang also had different patterns. The number of sites in different sub-regions over 1961–2013 for each type are shown in Figure 4. The total number of sites in north Xinjiang, Tianshan Mountains area, and south Xinjiang were 45, 17, and 43, respectively. The number of sites for the flat peak type were 11, 3, 7, and 21 in north Xinjiang, Tianshan Mountains area, south, and all of Xinjiang over the study period, respectively. The number of sites for the multi-peak type were 14, 6, 11, and 32 in north Xinjiang, Tianshan Mountains area, south, and all of Xinjiang, respectively. For the sharp single-peak type, the number of sites were 7, 1, 2, and 10 in north Xinjiang, Tianshan Mountains area, south,

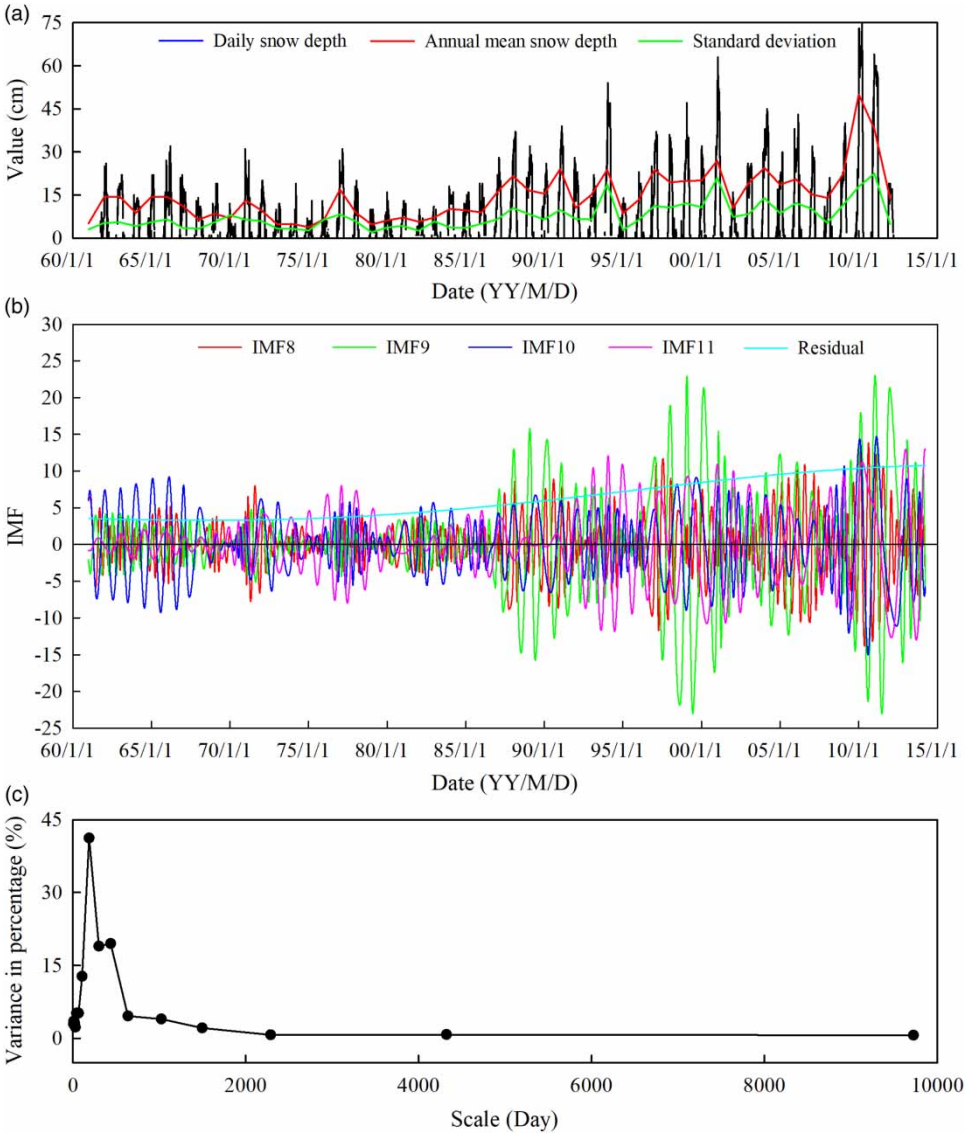


**Figure 2** | The observed (along with annual mean and standard error), IMFs and variance in percentage (decomposed by the EMD method) of daily snow depth at the Jimunai station over 1961–2013.

and all of Xinjiang, respectively. The number of sites for the right-skewed type were 12, 5, 7, and 25 in north Xinjiang, Tianshan Mountains area, south, and all of Xinjiang, respectively. In general, the variations of snow depth curve types in each sub-region fluctuated with a curve type order of multi-peak > right-skewed > flat peak > sharp single-peak.

In addition, based on the MMK trend test, the number of sites with flat peak and multi-peak types in north Xinjiang (Figure 4(a) and 4(b)) had significant increasing trends. The number of sites with sharp single-peak in north and all of Xinjiang (Figure 4(c)) had significant decreasing trends. The number of sites with multi-peak in north, south, and all of Xinjiang (Figure 4(b)), sharp single-peak in Tianshan Mountains area and south Xinjiang (Figure 4(c)), right-skewed in Tianshan Mountains area (Figure 4(d)), and flat peak in all of Xinjiang (Figure 4(a)) had insignificant increasing trends. Meanwhile, the number of sites with multi-peak in Tianshan Mountains area, right-skewed in north, south, and all of Xinjiang, and flat peak in Tianshan Mountains area and south

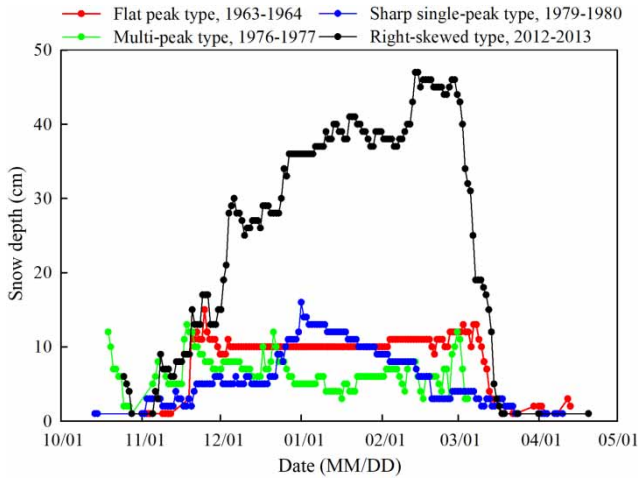


**Figure 3** | Four typical types of snow depth at the Jimunai station over 1961–2013.

Xinjiang had insignificant decreasing trends. These snow depth variation patterns were closely connected with temperature conditions.

## Temporal variations of snow cover parameters and their trends

Values of $D_s$, $D_e$, and $D_d$ in different sub-regions of Xinjiang over 1961–2013 are given in Table 1. The mean, maximal, and minimal $D_s$ values generally decreased from north to south. The mean $D_e$ decreased from north to south, and the maximal and minimal $D_e$ values in north Xinjiang and Tianshan Mountains area were generally larger than in south Xinjiang. $D_s$ and $D_e$ values in north Xinjiang were close to Tianshan Mountains area. The $D_d$ values ranged from 94 to 133 days for north Xinjiang, from 86 to 144 days for Tianshan Mountains area, and from 15 to 55 days for south Xinjiang, respectively. The mean $D_d$ values in the whole of Xinjiang were 96 days. The spatial distribution of $D_s$, $D_e$, and $D_d$ had a weak variability with $C_v$ values <0.1.

Figure 5 illustrates the temporal variations of annual $D_s$, $D_e$, and $D_d$ in different sub-regions of north Xinjiang, Tianshan Mountains area, south and all of Xinjiang. The annual variations of $D_s$ in north Xinjiang and Tianshan Mountains area were similar and generally earlier than south Xinjiang. The annual mean $D_s$ in south Xinjiang was November 30th, with the latest date on December 26th, 1973 and the earliest date on November 14th, 2000. The annual $D_e$ in north Xinjiang and Tianshan Mountains area had a similar range, both being later than south Xinjiang. The annual mean $D_e$ in south Xinjiang was March 5th, with the latest date on March 17th, 2010 and minimum date on February 17th, 1962. Consequently, the annual mean $D_d$ in north Xinjiang and Tianshan Mountains area was much longer than in south Xinjiang. The annual mean $D_d$ in south Xinjiang was 96 days, with a maximum of 120 days (in 1985), and a minimum of 71 days (in

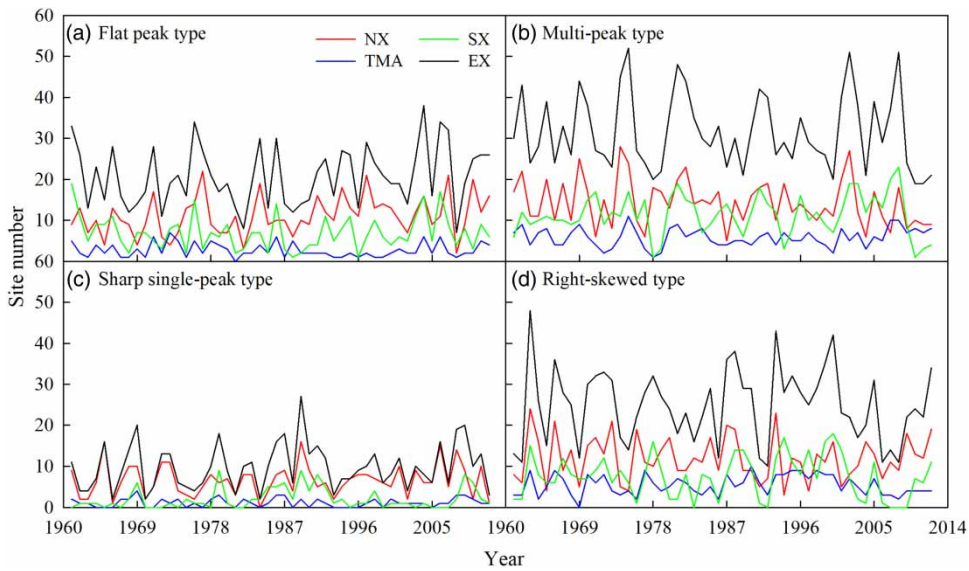


**Figure 4** | Number of sites with typical types for daily snow depth in different regions of Xinjiang over 1961–2013.

**Table 1** | Statistical properties of $D_s$, $D_e$, and $D_d$ in Xinjiang over 1961–2013

| Property | Sub-region | Mean | Maximum | Minimum | $\sigma$ | $C_v$ |
|---|---|---|---|---|---|---|
| $D_s$ | North Xinjiang | 144 | 164 | 128 | 7.72 | 0.054 |
| | Tianshan Mountains area | 147 | 164 | 127 | 9.28 | 0.063 |
| | South Xinjiang | 184 | 217 | 150 | 15.0 | 0.081 |
| | Entire Xinjiang | 154 | 179 | 137 | 8.76 | 0.057 |
| $D_e$ | North Xinjiang | 257 | 271 | 241 | 5.97 | 0.023 |
| | Tianshan Mountains area | 256 | 275 | 243 | 8.46 | 0.033 |
| | South Xinjiang | 219 | 240 | 193 | 10.3 | 0.047 |
| | Entire Xinjiang | 248 | 260 | 232 | 6.61 | 0.027 |
| $D_d$ (Day) | North Xinjiang | 113 | 133 | 94 | 9.74 | 0.086 |
| | Tianshan Mountains area | 109 | 144 | 86 | 12.9 | 0.118 |
| | South Xinjiang | 35 | 55 | 15 | 9.52 | 0.271 |
| | Entire Xinjiang | 96 | 120 | 71 | 11.1 | 0.117 |

*Note:* $D_s$, starting days counted from July 1st; $D_e$, end days counted from July 1st; $D_d$, snow cover duration; $\sigma$, standard deviation; $C_v$, variability coefficient.

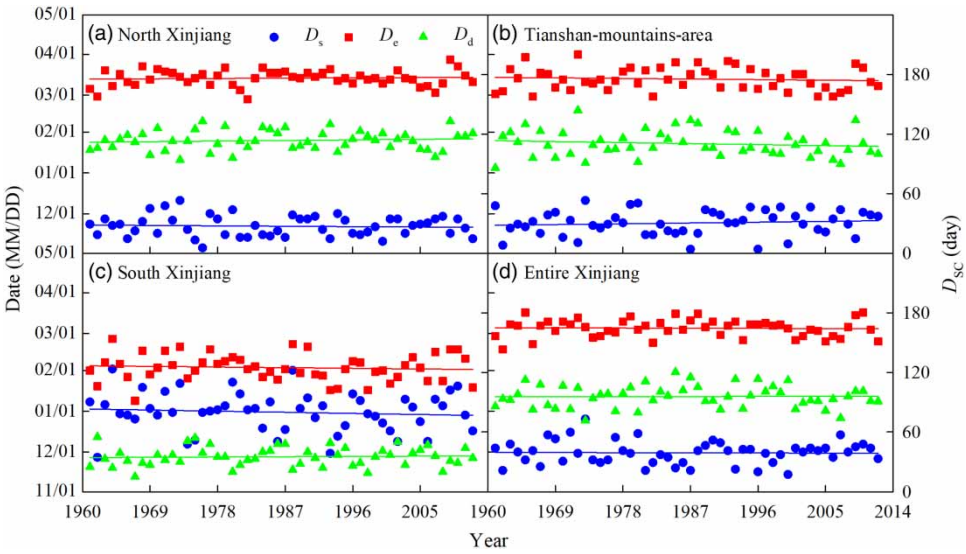


**Figure 5** | Temporal variations of the starting date ($D_s$), ending date ($D_e$) and snow cover duration ($D_d$) over 1961–2013 in different sub-regions of Xinjiang, China.

1995). Annual mean $D_s$ declined in north Xinjiang and south Xinjiang but increased in Tianshan Mountains area. In all of Xinjiang, annual mean $D_s$ showed a decreasing trend with a linear slope of 0.014 day/year. Annual mean $D_e$ declined in south Xinjiang and Tianshan Mountains area while it increased in north Xinjiang, and annual mean $D_e$ in all of Xinjiang showed a decreasing trend with a linear slope of 0.014 day/year. Annual mean $D_d$ increased in north Xinjiang and south Xinjiang while it declined in Tianshan Mountains area, and annual $D_d$ in all of Xinjiang had an increasing trend with a linear slope of 0.002 day/year. In general, the fluctuations of $D_s$, $D_e$, and $D_d$ were more abrupt in Tianshan Mountains area and south Xinjiang than in north Xinjiang, although their ranges were close, which showed that snow cover in north Xinjiang was more stable. Snow covered Xinjiang for about three months or longer. By the MMK trend test, $D_s$, $D_e$, and $D_d$ had insignificant increasing or decreasing trends. The Sen's slope ($b$) values ranged from $-0.03$ to 0.098 for $D_s$, from $-0.056$ to 0.029 for $D_e$, and from $-0.11$ to 0.03 for $D_d$ considering different sub-regions and all of Xinjiang. Different $b$ values for $D_s$ and $D_e$ resulted in various trends in $D_d$, although all $b$ values were small.

The temporal variations of annual $SD_{avr}$ and $SD_{max}$ in different sub-regions and four typical sites in Xinjiang are illustrated in Figure 6. The curves of $SD_{avr}$ decreased from north to south over the study period (Figure 6(a)), and $SD_{avr}$ showed an increase trend with a linear slope of 0.093, 0.054, 0.039, and 0.007 cm year$^{-1}$ in north Xinjiang the whole of Xinjiang, Tianshan Mountains area, and south Xinjiang, respectively. Among the four sites, Aletai and Jimunai belonged to north Xinjiang, Tianchi belonged to Tianshan Mountains area, and Luntai belonged to south Xinjiang. The variations of $SD_{avr}$ not only had regional features, but also were site-specific. $SD_{avr}$ decreased from north to south and ranking for sites was Aletai > Tianchi > Jimunai > Luntai (Figure 6(b)), and $SD_{avr}$ showed an increased trend with a linear slope of 0.267, 0.112, 0.365, and 0.021 cm/year in the above four stations, respectively. The ranges of $SD_{avr}$ varied from 0 to 53 cm for different sites across the region. $SD_{max}$ curves decreased from north to south (Figure 6(c)) and ranked as Aletai > Tianchi > Jimunai > Luntai (Figure 6(d)), similarly to $SD_{avr}$ variations. At either different sub-regions or the four typical sites, winter mean $SD_{max}$ had increasing trends. The ranges for $SD_{max}$ were much larger than $SD_{avr}$, which was reasonable. Other studies also showed that the $SD_{avr}$ in north Xinjiang was deeper than in south Xinjiang, and $SD_{max}$ in north Xinjiang (Fu *et al.* 2011). Our results agreed with theirs.

Further, the MMK trend test results showed that both $SD_{avr}$ or $SD_{max}$ had increasing trends, but the trends of $SD_{avr}$ in north, south, all of Xinjiang and at the sites Tianchi and Jimunai, and the trends of $SD_{max}$ in sub-regions of south and all of Xinjiang and at the sites Aletai, Tianchi, and Jimunai were insignificant. The $b$ values ranged from 0.02 to 057 decreasing from north to south and ranked as Jinunai > Aletai > Tianchi > Luntai for either $SD_{avr}$ or $SD_{max}$. This consistency in increasing trends of snow depth contributed to the overall increase of precipitation in Xinjiang, which has been reported by different studies (Shen *et al.* 2013; Li *et al.* 2017a).

## The spatial distributions of snow properties and their trends

The MKK statistic ($Z_m$) and Sen's slope ($b$) values for $D_s$, $D_e$, and $D_d$ were obtained for 105 sites throughout Xinjiang. The spatial distribution of multi-year mean $D_s$, $D_e$, and $D_d$ and their trend test results are shown in Figure 7. In Figure 7(a), $D_s$ showed clear regional differences between north and south Xinjiang with Tianshan Mountains area as a division, indicating much earlier snowfall in north than in south Xinjiang. For example, at Daxigou in Tianshan Mountains area, the earliest $D_s$ was October 1st, while at Baluntai in south Xinjiang, the latest $D_s$ was February 2nd. $D_s$ ranged from

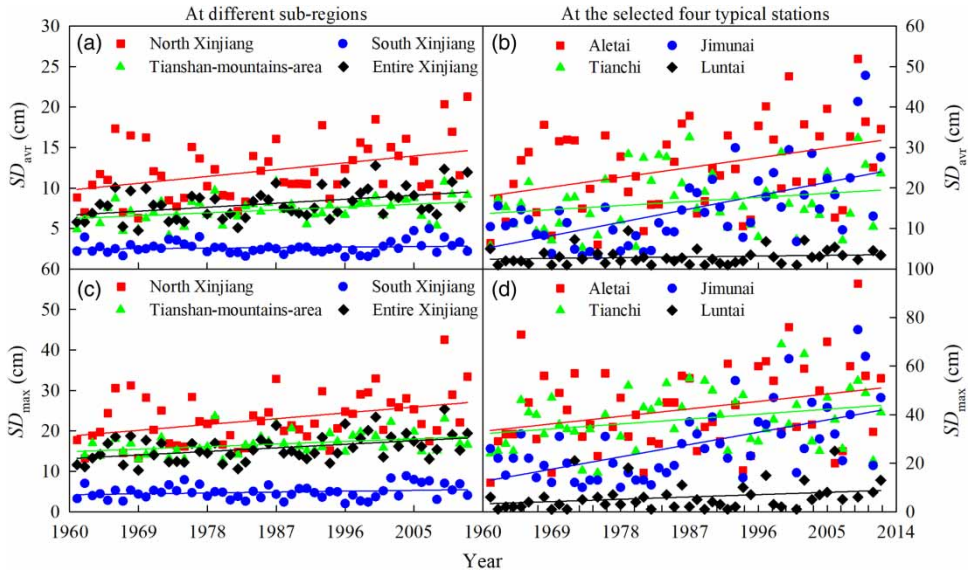


**Figure 6** | Variations of annual mean ($SD_{avr}$) and maximum snow depths ($SD_{max}$) over 1961–2013 in Xinjiang, China.

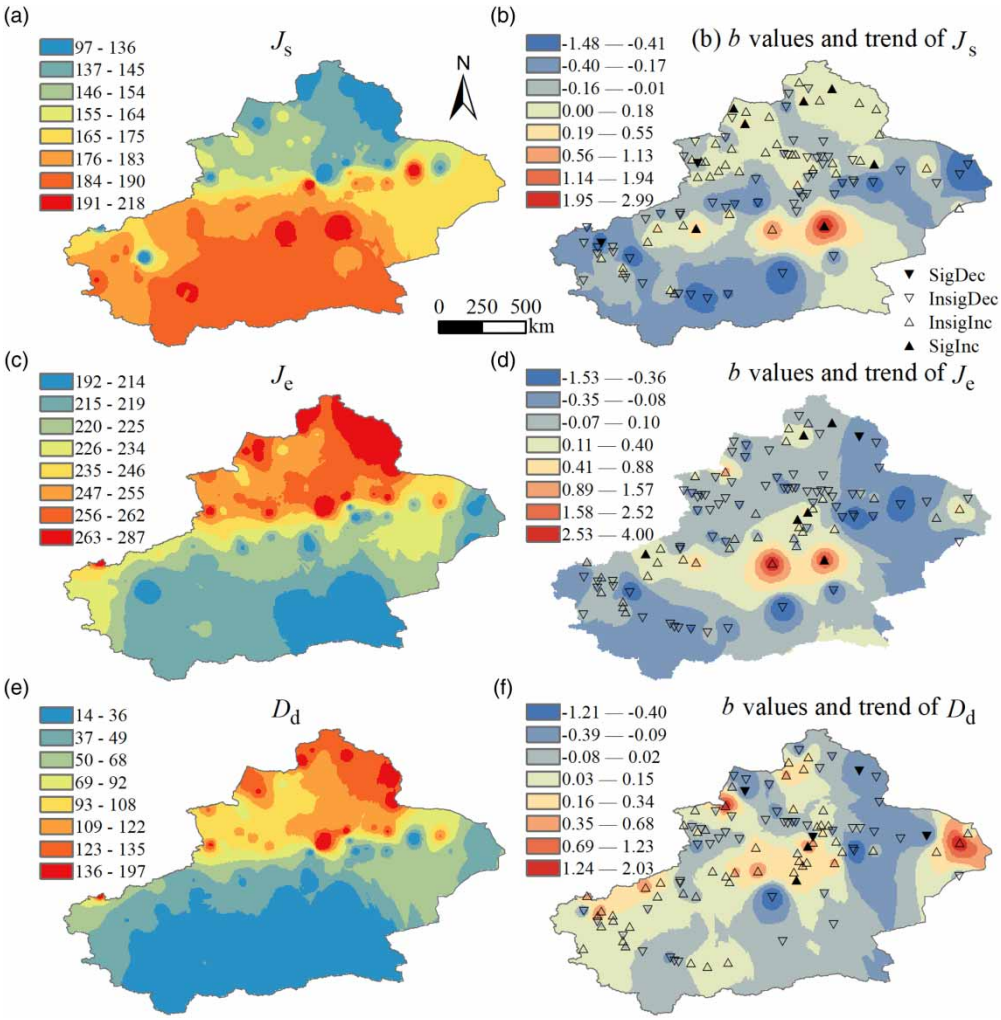


**Figure 7** | The spatial distribution of mean starting date ($D_s$), ending date ($D_e$), snow cover duration ($D_d$) and their trends over 1961–2013 in Xinjiang, China.

October 5th to November 29th in north Xinjiang and Tianshan Mountains area, while in south Xinjiang it ranged from December 12th to February 5th, respectively. This is due to the warm temperature or less snowfall in the dry winter there. In Figure 7(b), $D_s$ at 45 out of the total 105 sites had increasing trends, with $D_s$ being significant at seven sites. $D_s$ at the other 60 sites had decreasing trends, with $D_s$ at two sites being significant. Values of $b$ for $D_s$ varied from −1.5 to 3.0 across Xinjiang. In Figure 7(c) and 7(e), $D_e$ and $D_d$ also showed clear regional differences between north and south Xinjiang. $D_e$ ranged from February 18th to April 15th in north Xinjiang and Tianshan Mountains area while in south Xinjiang it ranged from January 9th to February 4th, respectively. Since snow started earlier and ended later in north Xinjiang than in south Xinjiang, as a consequence the $D_d$ values in north Xinjiang were much larger than in south Xinjiang. In Figure 7(d), $D_e$ at 34 sites had increasing trends, with $D_e$ at six sites being significant. $D_e$ at the other 71 sites had decreased trends, and only at one site was its trend significant. $D_d$ ranged from 74 to 199 in north Xinjiang and Tianshan Mountains area while in south Xinjiang it ranged from 14 to 46, respectively. In Figure 7(f), trends in $D_d$ at 53 sites increased, of which, trends at two sites were significant. Among the other 52 sites which had decreasing trends in $D_d$, trends at four sites were significant. Values of $b$ varied from −1.55 to 4.0 for $D_e$ and from −1.3 to 2.0 for $D_d$, respectively. $D_s$ at the 24 sites in north Xinjiang, eight sites in Tianshan Mountains

area, and 13 sites in south Xinjiang had increasing trends, while $D_e$ at the 36 sites in north Xinjiang, eight sites in Tianshan Mountains area and 24 sites in south Xinjiang had decreasing trends. $D_d$ at the 27 sites in north Xinjiang, seven sites in Tianshan Mountains area and 16 sites in south Xinjiang had increasing trends. Therefore, more sites in north Xinjiang had increased trends of $D_s$ and decreased trends of $D_e$ than in south Xinjiang. The number of sites with different trends in $D_s$, $D_e$, and $D_d$ for different subregions are given in Table 2. More sites had decreasing trends (e.g., $D_s$ in Tianshan Mountains area, south and all of Xinjiang, $D_e$ in north, south Xinjiang, and all of Xinjiang, and $D_d$ in north Xinjiang) than increasing trends.

The increasing $D_d$ may induce larger snow depth for the study sites. This may produce higher snow water equivalent and high discharge in Xinjiang. In the meantime, it may cause higher snowmelt flood risks when temperature increases rapidly within a very short period in spring. Therefore, the increase of $D_d$ in Xinjiang could be either beneficial or a threat for society and human safety.

Figure 8 shows the spatial distribution of multiyear mean monthly (in December, January, and February), annual mean $SD_{avr}$ and their trends. $SD_{avr}$ in all of the three months varied within 9.0 cm for south Xinjiang, but reached 17.7 cm in December, 29.3 cm in January, and 34.4 cm February for north Xinjiang, respectively. Similarly, the $b$ values had large variations in north Xinjiang and Tianshan Mountains area but much smaller variations in south Xinjiang, especially for the monthly data. The annual $SD_{avr}$ ranged between 5 and 25 cm in north Xinjiang and below 6 cm in south Xinjiang. Eighty-six sites had increasing trends in annual $SD_{avr}$, of which trends at 16 sites were significant; among the other 19 sites with decreasing trends, trends at two sites were significant. Annual $SD_{avr}$ at 41 sites in north Xinjiang, 16 sites in Tianshan Mountains area and 29 sites in south Xinjiang had increasing trends. Therefore, most sites in all of Xinjiang had increasing trends in annual $SD_{avr}$ (Table 2).

Figure 9 shows the spatial distribution of multiyear mean monthly $SD_{max}$, annual mean $SD_{max}$ and their trends. Also similar to $SD_{avr}$, $SD_{max}$ varied little in the south but greatly in north Xinjiang and Tianshan Mountains area. The values of $b$ varied in December, January, and February, and the annual scale in all of Xinjiang. The annual $SD_{max}$ ranged between 24 and 95 cm in north Xinjiang and below 33 cm in south Xinjiang, respectively. The smallest $SD_{avr}$ and $SD_{max}$ were in the Taklamakan desert zone. Ninety sites had increasing trends in annual $SD_{max}$, of which, trends at 18 sites were significant, while the other 15 sites had insignificant decreasing trends. $SD_{max}$ at the

**Table 2** | The number of sites with different trends of monthly and annual snow properties in north Xinjiang, TMA, south, and the whole of Xinjiang

| | | | | | $SD_{avr}$ | | | | $SD_{max}$ | | | |
|---|---|---|---|---|---|---|---|---|---|---|---|---|
| **Region** | **Trend** | $D_s$ | $D_e$ | $D_d$ | **Dec** | **Jan** | **Feb** | **Annual** | **Dec** | **Jan** | **Feb** | **Annual** |
| North Xinjiang | SigDec | 1 | 1 | 2 | 0 | 0 | 0 | 2 | 0 | 0 | 0 | 0 |
| | InsigDec | 20 | 35 | 25 | 2 | 2 | 4 | 2 | 2 | 2 | 2 | 2 |
| | SigInc | 20 | 7 | 18 | 29 | 16 | 26 | 31 | 23 | 17 | 22 | 29 |
| | InsigInc | 4 | 2 | 0 | 14 | 27 | 15 | 10 | 20 | 26 | 21 | 14 |
| Tianshan Mountains area | SigDec | 0 | 0 | 2 | 0 | 0 | 0 | 0 | 0 | 0 | 0 | 0 |
| | InsigDec | 9 | 8 | 5 | 3 | 1 | 2 | 1 | 3 | 2 | 2 | 1 |
| | SigInc | 7 | 6 | 9 | 11 | 13 | 11 | 14 | 11 | 13 | 10 | 13 |
| | InsigInc | 1 | 3 | 1 | 3 | 3 | 4 | 2 | 3 | 2 | 5 | 3 |
| South Xinjiang | SigDec | 1 | 0 | 0 | 0 | 0 | 0 | 0 | 0 | 0 | 0 | 0 |
| | InsigDec | 29 | 24 | 16 | 10 | 11 | 18 | 14 | 9 | 14 | 18 | 12 |
| | SigInc | 11 | 18 | 26 | 33 | 32 | 24 | 25 | 32 | 29 | 24 | 30 |
| | InsigInc | 2 | 1 | 1 | 0 | 0 | 1 | 4 | 2 | 0 | 1 | 1 |
| Entire Xinjiang | SigDec | 2 | 1 | 4 | 0 | 0 | 0 | 2 | 0 | 0 | 0 | 0 |
| | InsigDec | 58 | 67 | 46 | 15 | 14 | 24 | 17 | 14 | 18 | 22 | 15 |
| | SigInc | 38 | 31 | 53 | 73 | 61 | 61 | 70 | 66 | 59 | 56 | 72 |
| | InsigInc | 7 | 6 | 2 | 17 | 30 | 20 | 16 | 25 | 28 | 27 | 18 |

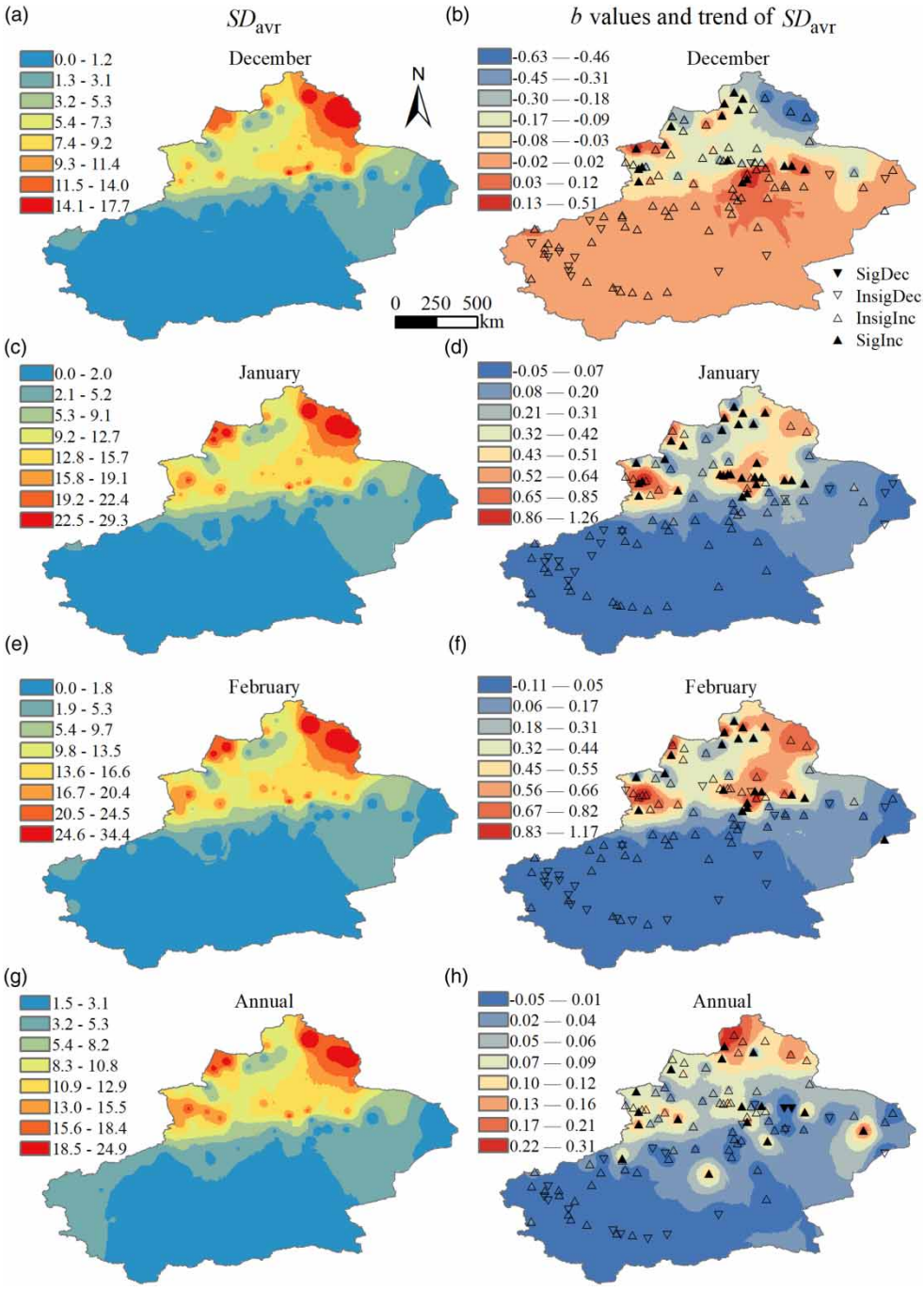


**Figure 8** | Trends and the spatial distribution of monthly (in December, January and February) and annual mean snow depth ($SD_{avr}$) over 1961–2013 in Xinjiang, China.

43 sites in north Xinjiang, 16 sites in Tianshan Mountains area and 31 sites in south Xinjiang had increasing trends. Similar to annual $SD_{avr}$, most sites in all of Xinjiang had increasing trends in annual $SD_{max}$ (Table 2).

The number of sites in Table 2 corresponding to Figures 6–8 show that most sites in different sub-regions had increasing trends in the studied snow properties; many less sites had significant decreasing trends. As

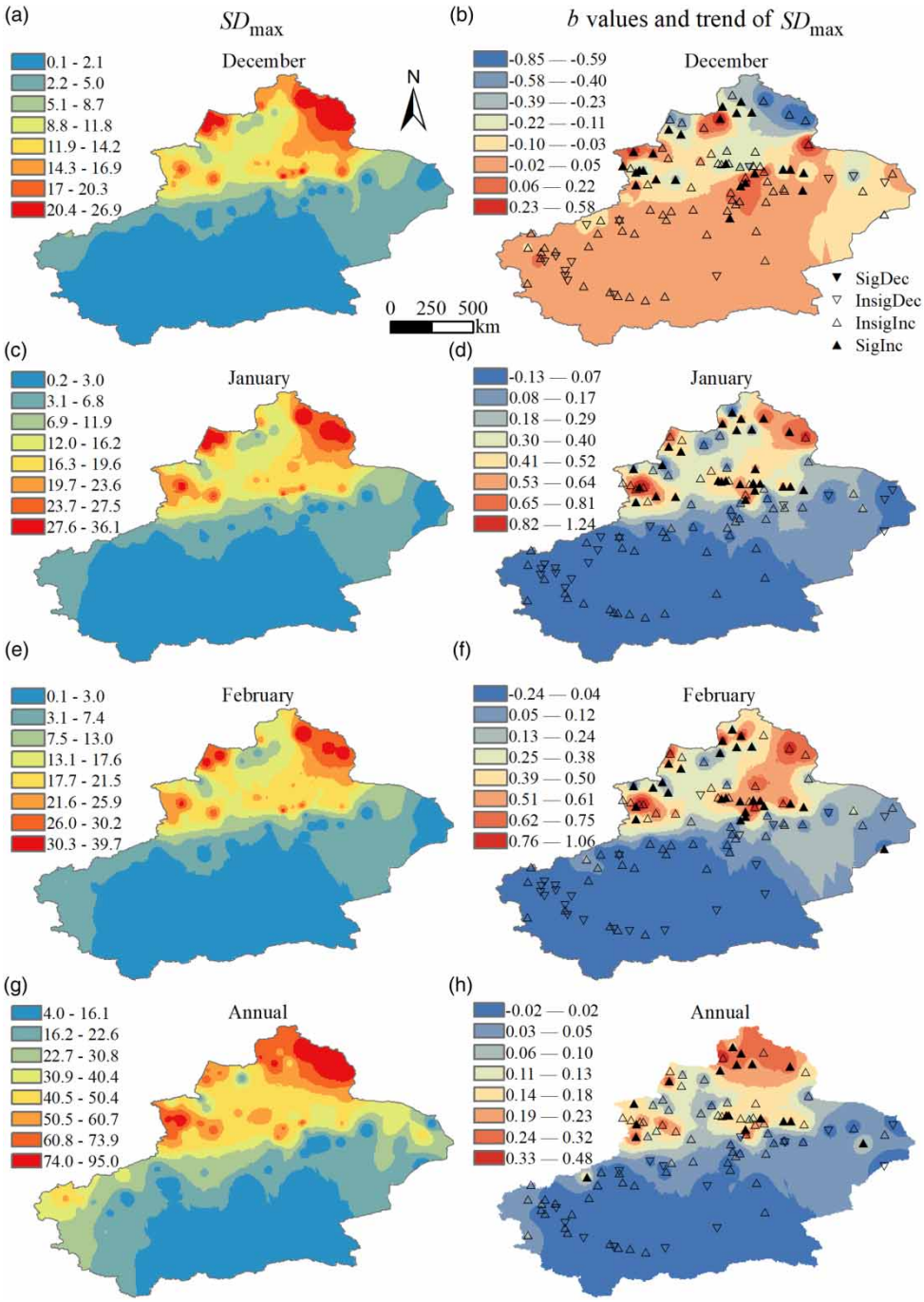


**Figure 9** | Trends and the spatial distribution of monthly (in December, January and February) and annual maximum snow depth ($SD_{max}$) over 1961–2013 in Xinjiang, China.

mentioned above, the increases in $SD_{avr}$ and $SD_{max}$ reflect the increase in precipitation, which is consistent with Li *et al.* (2017b) who showed generally increasing precipitation over 1961–2013 in Xinjiang, China. Both $SD_{avr}$ and $SD_{max}$ had seasonality.

## The EOF and EC of daily snow depth

The variance percentage for each EOF was obtained. EOF1, EOF2, EOF3, and EOF4 was 70.0%, 6.7%, 4.0%, and 2.4%, accounting for 83.1% of the total spatial

variability, of which, only EOF1 was significant at the 95% confidence level. Although EOF2 through EOF10 were insignificant, the total variation explained by these patterns was about 20%, which implied that about one-fifth of the spatial variation in snow depth was random in time and did not belong to a temporary correlated spatial pattern. Therefore, Figure 10 shows the EOF1 and EC1 that explain the most variation. As shown in Figure 10(a), the values of EOF1 were negative for south Xinjiang but positive for north Xinjiang, indicating the differences of snow depth in space, which could be caused by the climatic conditions. Absolute values of EOF1 in north Xinjiang were larger than in south Xinjiang, which indicated that snow depth in north Xinjiang varied more. In Figure 10(b), the EC1 values fluctuated with the years and had obvious periods but no typical trends.

## CONCLUSIONS

Spatiotemporal characteristics of snow properties, including starting and ending date of snow cover, snow depth, and snow cover duration in Xinjiang, China, were investigated. For the temporal variations, the annual mean starting date ranged from November 15th to December 27th. The annual mean ending date ranged from February 17th to March 16th. The annual snow cover duration lasted for 71 to 120 days. Both the average and maximum snow depths fluctuated and decreased from north to south. Four typical types of daily snow depth within the snow-cover year, i.e., flat peak, multi-peak, sharp single-peak, and right-skewed, were generalized. Among the 17 IMFs and residual generated by the empirical mode decomposition (EMD), about half- and one-year scales were demonstrated by IMF10, IMF11, and IMF12.

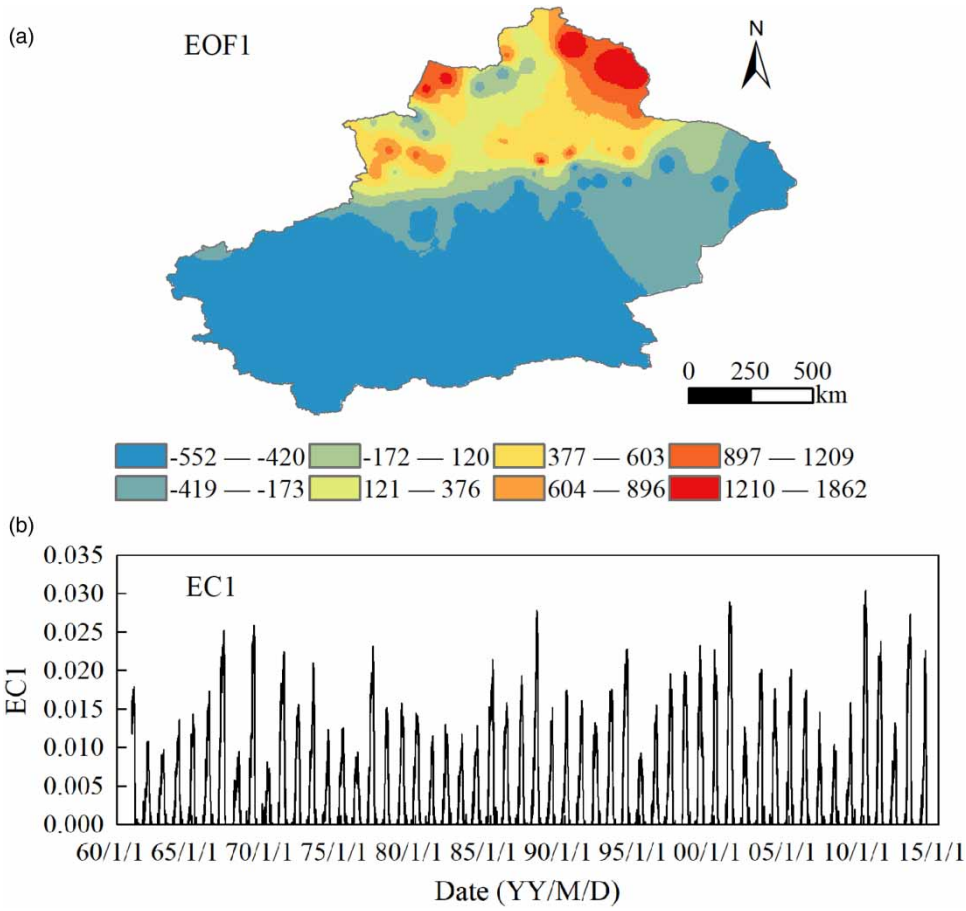


**Figure 10** | The EOF1 and EC1 for daily snow depth in Xinjiang over 1961–2013.

For the spatial distributions, starting (ending) date values delayed (advanced) but snow depth values decreased from north to south Xinjiang. Average and winter maximum snow depth were much larger in Tianshan Mountains area and north Xinjiang than in south Xinjiang. Starting date increased from October 5th to February 5th, while ending date, snow cover duration, average and winter maximum snow depths decreased and ranged from January to April, 14–199 days, 1.5–24.9 cm, and 4.0–95.0 cm, respectively. The MMK test showed that, starting date at 60 sites had decreasing trends, of which, trends at two sites were significant; moreover, seven out of the other 45 sites for starting date had significant increasing trends. Trends of ending date at 71 and 34 sites decreased and increased, respectively, of which, trends at one and six sites were significant, respectively. Fifty-two and 53 sites had decreasing and increasing trends in snow cover duration, of which, trends at four and two sites were significant, respectively. Nineteen (86) sites had decreasing (increasing) trends in annual average snow depth, of which, trends at three and 22 sites were significant, respectively. As to winter maximum snow depth, 15 and 90 sites had decreasing and increasing trends, of which, trends at none and 25 sites were significant, respectively. The first empirical orthogonal function (EOF1) accounted for 79% of the spatial variability in snow depth, of which, larger variability was shown for north than south Xinjiang.

Seasonality of the monthly average and maximum snow depths were shown by comparing data series in December, January, and February. Further studies for snow density are needed in future research, to clearly reveal how snow-water equivalent varies in Xinjiang, China.

## ACKNOWLEDGEMENTS

This research was financially supported by China National Science Foundations (No. U1203182 and 51579213), and the China 111 project (B12007). We thank the three anonymous reviewers who provided many helpful comments which helped improve the manuscript.

## REFERENCES

Bavay, M., Lehning, M., Jonas, T. & Löwe, H. 2009 Simulations of future snow cover and discharge in Alpine headwater catchments. *Hydrological Processes* **23** (1), 95–108. DOI: 10.1002/hyp.7195.

Butt, M. J. 2006 Passive microwave methods to retrieve snow pack characteristics in the UK. *Scottish Geographical Journal* **122** (1), 19–31. DOI: 10.1080/00369220600830797.

Butt, M. J. & Kelly, R. E. J. 2008 Estimation of snow depth in the UK using the HUT snow emission model. *International Journal of Remote Sensing* **29** (14), 4249–4267. DOI: 10.1080/01431160801891754.

Cerrone, D., Fusco, G. & Cotroneo, Y. 2017 The Antarctic circumpolar wave: its presence and interdecadal changes during the last 142 years. *Journal of Climate* **30** (16), 6371–6389.

Chen, C. X., Li, Y. & Li, Q. H. 2015 Snow cover depth in Urümqi region, Xinjiang: evolution and response to climate change. *Journal of Glaciology and Geocryology* **37** (3), 587–594 (in Chinese with English abstract). DOI: 10.7522/j.issn.1000-0240.2015.0066.

Deepthi, A., Siegfried, D. S. & Yury, V. V. 2017 North Pacific decadal variability: insights from a biennial ENSO environment. *Climate Dynamics* **49** (4), 1379–1397.

Dey, B. & Kumar, O. B. 1983 Himalayan winter snow cover area and summer monsoon rainfall over India. *Journal of Geophysical Research Oceans* **88** (C9), 5471–5474. DOI: 10.1029/JC088iC09p05471.

Foster, J., Owe, M. & Rango, A. 1983 Snow cover and temperature relationship in North America and Eurasia. *Journal of Applied Meteorology and Climatology* **22** (3), 460–469. DOI: 10.1175/1520-0450(1983)022 < 0460:SCATRI > 2.0.CO;2.

Frei, A. & Gong, G. 2005 Decadal to century scale trends in North American snow extent in coupled atmosphere-ocean general circulation models. *Geophysical Research Letters* **32** (18), 109–127. DOI: 10.1029/2005GL023394.

Frei, A. & Robinson, D. A. 1999 Northern hemisphere snow extent: regional variability 1972–1994. *International Journal of Climatology* **19** (14), 1535–1560. DOI: 10.1002/(SICI)1097-0088(19991130)19:14 < 1535::AID-JOC438 > 3.0.CO;2-J.

Fu, C. B., Dan, L. & Wu, J. 2011 The distribution of snow depth snow pressure in Xinjiang and their variation characteristics in 55 years. *Progress in Geophysics* **26** (1), 182–193 (in Chinese with English abstract).

Goovaerts, P. 1998 Geostatistical tools for characterizing the spatial variability of microbiological and physico-chemical soil properties. *Biology and Fertility of Soils* **27**, 315–334. doi:10.1007/s003740050439.

Grody, N. C. & Basist, A. N. 1996 Global identification of snowcover using SSM/I measurements. *IEEE Transactions on Geoscience & Remote Sensing* **34** (1), 237–249. DOI: 10.1109/36.481908.

Hahn, D. G. & Shukla, J. 1976 An apparent relationship between Eurasian snow cover and Indian monsoon rainfall. *Journal of the Atmospheric Sciences* **33** (12), 2461–2462.

Hardoon, D. R., Szedmak, S. & Shawe-Yaylor, J. 2004 Canonical correlation analysis: an overview with application to learning methods. *Neural Computation* **16**, 2639–2664.

Helsel, D. R. & Hirsch, R. M. 2002 *Statistical Methods in Water Resources.* Elsevier, Amsterdam, New York

Hu, W. & Si, B. C. 2016 Estimating spatially distributed soil water content at small watershed scales based on decomposition of temporal anomaly and time stability analysis. *Hydrology and Earth System Sciences* **20**, 571–587. doi:10.5194/hess-20-571-2016.

Hu, W., Chau, H. W., Qiu, W. & Si, B. 2017 Environmental controls on the spatial variability of soil water dynamics in a small watershed. *Journal of Hydrology* **551**, 47–55.

Jin, J. M. & Wen, L. J. 2012 Evaluation of snowmelt simulation in the weather research and forecasting model. *Journal of Geophysical Research Atmospheres* **117** (D10), 10110. DOI: 10.1029/2011jd016980.

Kendall, M. G. 1975 *Rank Auto-Correlation Methods.* Charles Griffin, London.

Kottegoda, N. T. 1980 *Stochastic Water Resources Technology.* Palgrave Macmillan, pp. 396. DOI: 10.1007/978-1-349-03467-3.

Lamb, H. H. 1955 Two-way relationship between the snow or ice limit and 1000-500 mb thickness in the overlying atmosphere. *Quarterly Journal of the Royal Meteorological Society* **81** (348), 172–189. DOI: 10.1002/qj.49708134805.

Li, P. J. & Mi, D. S. 1983 Distribution of snow cover in China. *Journal of Glaciology and Geocryology* **5** (4), 9–18 (in Chinese with English abstract).

Li, Y., Horton, R., Ren, T. S. & Chen, C. Y. 2010 Prediction of annual reference evapotranspiration using climatic data. *Agricultural Water Management* **97** (2), 300–308. DOI: 10.1016/j.agwat.2009.10.001.

Li, Y., Chen, C. Y. & Sun, C. F. 2017a Drought severity and change in northwestern China over 1961–2013. *Hydrology Research* **48** (1). DOI: 10.2166/nh.2016.026.

Li, Y., Yao, N., Sahin, S. & Appels, W. A. 2017b Spatiotemporal variability of four precipitation-based drought indices in Xinjiang, China. *Theoretical and Applied Climatology* **129** (3), 1017–1034. DOI: 10.1007/s00704-016-1827-5.

Liston, G. E. 1999 Interrelationships among snow distribution, snowmelt, and snow cover depletion: implications for atmospheric, hydrologic and ecological modeling. *Journal of Applied Meteorology and Climatology* **38** (10), 1474–1487. DOI: 10.1175/1520-0450(1999)038 < 1474:IASDSA > 2.0.CO;2.

Mann, H. B. 1945 Non-parametric tests against trend. *Journal of the Econometric Society* **13** (3), 245–259.

Namias, J. 1964 Seasonal persistence and recurrence of European blocking during 1958–1960. *Tellus* **16** (3), 394–407.

Nauditt, A., Birkel, C., Soulsby, C. & Ribbe, L. 2017 Conceptual modelling to assess the influence of hydro-climatic variability on runoff processes in data scarce semi-arid Andean catchments. *Hydrological Sciences Journal* **62** (4), 515–532.

Nielsen, D. R. & Bouma, J. 1985 Soil spatial variability. In: *Proceedings of a Workshop of the ISSS and the SSSA*, Las Vegas, USA, 30 November–1 December, 1984, Pudoc Wageningen, pp. 243.

North, G. R., Bell, T. L., Cahalan, R. F. & Moeng, F. J. 1982 Sampling errors in the estimation of empirical orthogonal functions. *Monthly Weather Review* **110** (7), 699–706.

Perry, M. A. & Niemann, J. D. 2007 Analysis and estimation of soil moisture at the catchment scale using EOFs. *Journal of Hydrology* **334**, 388–404.

Pomeroy, J. W., Gray, D. M., Brown, T., Hedstrom, N. H., Quinton, W. L., Granger, R. J. & Carey, S. K. 2007 The cold regions hydrological model: a platform for basing process representation and model structure on physical evidence. *Hydrological Processes* **21** (19), 2650–2667. DOI: 10.1002/hyp.6787.

Rango, A., Martinec, J., Chang, A. T. C., Foster, J. L. & van Katwijk, V. F. 1989 Average areal water equivalent of snow in a mountain basin using microwave and visible satellite data. *IEEE Transactions on Geoscience and Remote Sensing* **27** (6), 740–745. DOI: 10.1109/36.35962.

Rott, H. & Nagler, T. 1995 Intercomparison of snow retrieval algorithms by mean of space borne microwave radiometry. In: *Passive Microwave Remote Sensing of Land-Atmosphere Interaction* (B. J. Choudhury, Y. H. Kerr, E. G. Njoki & P. Pampaloni, eds). VSP, Utrecht, The Netherlands, pp. 227–243.

Sen, P. K. 1968 Estimates of the regression coefficient based on Kendall's tau. *Journal of American Statistical Association* **63** (324), 1379–1389.

Shen, Y. P., Su, H. C. & Wang, G. Y. 2013 The response of glaciers and snow cover to climate change in Xinjiang (II): hazards effects. *Journal of Glaciology and Geocryology* **35** (6), 1355–1370 (in Chinese with English abstract).

Sung, E. K., Won, S. & Soo, Y. C. 2017 Assessment of water quality variation of a monitoring network using exploratory factor analysis and empirical orthogonal function. *Environmental Modelling & Software* **94**, 21–35. https://doi.org/10.1016/j.envsoft.2017.03.035.

Tait, A. & Armstrong, R. 1996 Evaluation of SMMR satellite-derived snow depth using ground-based measurements. *International Journal of Remote Sensing* **17** (4), 657–665. DOI: 10.1080/01431169608949036.

Tang, X. L., Lv, X. & He, Y. 2013 Features of climate change and their effects on glacier snow melting in Xinjiang, China. *Comptes Rendus Geoscience* **345** (2), 93–100. DOI: 10.1016/j.crte.2013.01.005.

Topaloglu, F. 2006 Regional trend detection of Turkish river flows. *Hydrology Research* **37** (2), 165–182. DOI: 10.2166/Nh.2006.006.

Wang, J. R., Chang, A. T. C. & Sharma, A. K. 1992 On the estimation of snow depth from microwave radiometric measurements. *IEEE Transactions on Geoscience and Remote Sensing* **30** (4), 785–791. DOI:10.1109/36.158873.

Wang, H. W., Huang, C. L., Hao, X. H., Zhang, P. & Hou, J. L. 2014 Analyses of the spatiotemporal variations of snow cover in North Xinjiang. *Journal of Glaciology and Geocryology* **36** (3), 508–516 (in Chinese with English abstract). DOI: 10.7522/j.issn.1000-0240.2014.0061.

Wang, C., Yang, K. & Li, Y. 2017 Impacts of spatiotemporal anomalies of Tibetan Plateau snow cover on summer precipitation in eastern China. *Journal of Climate* **30** (3), 885–903.

Wu, R. G. & Kirtman, B. P. 2007 Observed relationship of spring and summer East Asian rainfall with winter and spring Eurasian snow. *Journal of Climate* **20** (7), 1285–1304. DOI: 10.1175/JCLI4068.1.

Yang, P., Xia, J., Zhan, C., Qiao, Y. & Wang, Y. 2017 Monitoring the spatio-temporal changes of terrestrial water storage using GRACE data in the Tarim River basin between 2002 and 2015. *Science of The Total Environment* **595**, 218–228. https://doi.org/10.1016/j.scitotenv.2017.03.268.

Yue, S. & Wang, C. Y. 2002 Regional streamflow trend detection with contribution of both temporal and spatial auto-correlation. *International Journal of Climatology* **22** (8), 933–946. DOI: 10.1002/joc.781.

First received 26 February 2017; accepted in revised form 20 November 2017. Available online 11 December 2017